

Neuronal fate determinants of adult olfactory bulb neurogenesis

Michael A Hack^{1,6}, Armen Saghatelian^{2,6}, Antoine de Chevigny², Alexander Pfeifer³, Ruth Ashery-Padan⁴, Pierre-Marie Lledo² & Magdalena Götz^{1,5}

Adult neurogenesis in mammals is restricted to two small regions, including the olfactory bulb, where GABAergic and dopaminergic interneurons are newly generated throughout the entire lifespan. However, the mechanisms directing them towards a specific neuronal phenotype are not yet understood. Here, we demonstrate the dual role of the transcription factor Pax6 in generating neuronal progenitors and also in directing them towards a dopaminergic periglomerular phenotype in adult mice. We present further evidence that dopaminergic periglomerular neurons originate in a distinct niche, the rostral migratory stream, and are fewer derived from precursors in the zone lining the ventricle. This regionalization of the adult precursor cells is further supported by the restricted expression of the transcription factor Olig2, which specifies transit-amplifying precursor fate and opposes the neurogenic role of Pax6. Together, these data explain both extrinsic and intrinsic mechanisms controlling neuronal identity in adult neurogenesis.

Recent progress shows not only that neurons suitable for transplantation can be generated from embryonic or adult neural stem cells maintained in culture, but also that the adult brain itself produces new cells capable of regenerating functional neurons in diseased areas^{1,2}. These findings raise new hope for development of cell therapy in neurodegenerative disorders, but they require a thorough understanding of the mechanisms directing adult neural stem cells toward specific neuronal phenotypes.

Neurogenesis supplying the adult olfactory bulb is an excellent system in which to study these mechanisms, as two distinct types of interneurons are continuously generated throughout adulthood^{3–5}: neurons located in the granule cell layer (GCL) inside the olfactory bulb (granule neurons), and a diverse set of neurons in the outer region of the olfactory bulb, in the glomerular layer (Fig. 1a,b). Granule neurons are homogeneously GABAergic, whereas of the periglomerular neurons in the glomerular layer, only 40% are GABAergic, and of those, 65% are dopaminergic⁶. The remaining periglomerular neurons contain either calretinin or calbindin^{7–9}. Normally, the majority of newly generated neurons are granule neurons, with only a small proportion acquiring a periglomerular neuron fate⁷. However, the molecular mechanisms that specify these neuronal subtypes in the appropriate composition are still unknown.

During development, the fate of neuronal subtypes is specified in the precursor cells by a precise transcription factor code along the dorsoventral and rostrocaudal axes¹⁰. This principle also seems to apply to

the developing telencephalon, where distinct dorsoventral domains generate distinct types of neurons^{11–13}. It is not clear whether the concept of regional specification of neuronal subtypes might also apply for adult neurogenesis, because dorsoventral patterning is less obvious in the adult brain, as massive cell type mixing occurs postnatally in the subependymal zone (SEZ)¹⁴. In fact, adult olfactory bulb neurogenesis has so far been perceived as a single lineage originating from astroglia-like stem cells immunoreactive for glial fibrillary acidic protein (GFAP; type B cells) lining the lateral wall of the lateral ventricle (Fig. 1c,d^{15,16}). These adult neural stem cells divide slowly, whereas their progeny, the transit-amplifying precursors (type C cells)^{15–18}, divide fast and generate neuronal precursors (type A cells) that already express neuronal traits such as PSANCAM or doublecortin and migrate through the rostral migratory stream (RMS) towards the olfactory bulb^{4,5} (Fig. 1c,d). However, when and how this lineage diverges to generate distinct types of neurons is not known.

Here we demonstrate that Pax6 upholds adult olfactory bulb neurogenesis by promoting the generation of neuronal progenitors and directing them towards the dopaminergic periglomerular phenotype. By contrast, Olig2 specifies the transit-amplifying precursor fate, opposes the neurogenic role of Pax6 and promotes oligodendrogenesis. We further show that dopaminergic periglomerular neurons are predominantly generated in the RMS, highlighting intrinsic and extrinsic mechanisms governing fate determination in adult neurogenesis.

¹GSF-National Research Center for Environment and Health, Institute for Stem Cell Research, Ingolstädter Landstr. 1, D-85764 Neuherberg, Germany. ²Laboratory of Perception and Memory, Centre National de la Recherche Scientifique, Unité de Recherche Associée 2182, Pasteur Institute, 25 rue du Dr. Roux, 75724 Paris Cedex 15, France. ³Molecular Pharmacology, Department of Pharmacy, Center for Drug Research, Ludwig-Maximilians-Universität München, Butenandtstr. 5-13, 81377 Munich, Germany. ⁴Department of Human Genetics and Molecular Medicine, Sackler Faculty of Medicine, Ramat Aviv, Tel Aviv 69987 Israel. ⁵Institute of Physiology, University of Munich, Pettenkoferstr. 12, 80336 Munich, Germany. ⁶These authors contributed equally to this work. Correspondence should be addressed to M.G. (magdalena.goetz@gsf.de) or P.-M.L. (pmlledo@pasteur.fr).

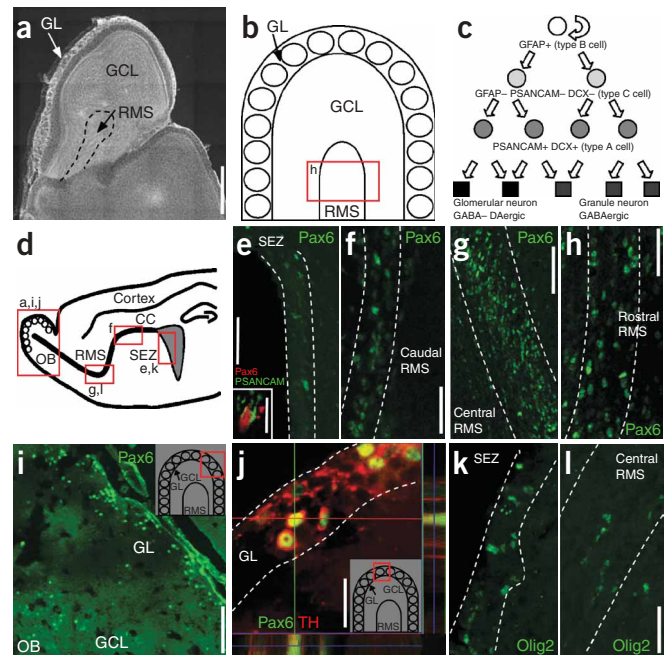
Figure 1 Expression of the transcription factors Pax6 and Olig2 in the SEZ-olfactory bulb pathway. **(a)** Micrograph of a DAPI-labeled section of the olfactory bulb (rostral up, caudal down, dorsal right, ventral left). **(b)** Schematic drawing of section in **a** with same orientation. **(c)** Schematic drawing illustrating the lineage and cell type markers of adult neural precursors. **(d)** Schematic drawing of a sagittal section of an adult mouse brain depicting the localization of the micrographs in **a,e,f,g,i,j,k,l** (red boxes). **(e–j)** Micrographs of Pax6-immunopositive cells at different rostrocaudal levels in the SEZ and RMS. Inset in **e**: PSANCAM immunostaining in green, Pax6 in red. TH, tyrosine hydroxylase. Panel **j** shows micrographs of the z-stack of the confocal picture along the y-axis (right) and the x-axis (left). Insets in **i** and **j** show localization of the micrographs. **(k,l)** Micrographs of Olig2-immunoreactive cells. SEZ: subependymal zone, RMS: rostral migratory stream, CC: corpus callosum, OB: olfactory bulb, GL: glomerular layer, GCL: granule cell layer, DCX, doublecortin. Scale bars: **a**, 500 μ m; **e,f,h,k,l**, 60 μ m (4 μ m for the inset); **g,i**: 150 μ m; **j**: 20 μ m.

RESULTS

Localization of Pax6 and Olig2 in the SEZ-olfactory bulb pathway

As described above, the apparent coexistence of Olig2 and Pax6 in the adult SEZ prompted us to examine their exact spatial location, as these transcription factors do not occur in the same domain of the developing telencephalon. Indeed, the localization of Pax6 and Olig2 in adult neural precursors revealed a marked difference along the rostrocaudal extension of the SEZ-RMS system that had previously not been noticed (**Fig. 1e,f,g,h,k,l**). The number of Pax6-immunostained cells was lowest in the region lining the ventricle, where only $7 \pm 3\%$ of DAPI-labeled cells were Pax6-positive ($n = 223$, three animals; **Fig. 1e**). In the caudal RMS immediately adjacent to the SEZ, however, the proportion of Pax6-immunopositive cells increased to $40 \pm 4\%$ ($n = 167$, three animals; **Fig. 1f**) with a further increase to $61 \pm 5\%$ ($n = 221$, three animals; **Fig. 1g**) in the central RMS, where the descending limb of the RMS intersects with the horizontal limb. The number of Pax6-positive cells then decreased when cells reach the olfactory bulb ($25 \pm 3\%$ of DAPI-labeled nuclei are Pax6-positive inside the RMS in the olfactory bulb; $n = 162$, two animals; **Fig. 1h**) and only a few Pax6-immunopositive cells were scattered throughout the olfactory bulb (**Fig. 1i**). The same distribution was also observed at the mRNA level (data not shown).

Within this expression gradient, Pax6 is found in similar cell types. Most of the Pax6-positive cells were migrating neuroblasts, as shown by PSANCAM or doublecortin (DCX) immunostaining throughout the SEZ and RMS (SEZ: $74 \pm 4\%$ of Pax6-positive cells were DCX-positive, $n = 235$, two animals; RMS: $67 \pm 5\%$, $n = 563$, two animals). We did not detect colocalization of Pax6 and GFAP at any position ($< 1\%$, $n = 142$, three animals). Thus, Pax6-positive cells are mostly neuroblasts, and one-third are precursors at a less committed stage throughout the SEZ-RMS system. There was a notable accumulation of Pax6-positive cells in the glomerular layer (**Fig. 1i**), where most Pax6-immunoreactive cells had differentiated into postmitotic neurons ($83 \pm 7\%$ of Pax6-positive cells were NeuN-positive, $n = 228$, three animals). In contrast, hardly any of the Pax6-positive cells in the GCL were NeuN-positive ($11 \pm 4\%$, $n = 341$, three animals), suggesting that Pax6 is downregulated in differentiating granule neurons, but not in periglomerular neurons. In the glomerular layer, Pax6 is mostly expressed in tyrosine hydroxylase (TH)-immunopositive neurons (**Fig. 1j**; 78% of Pax6-positive cells in the glomerular layer were TH-positive, and 95% of TH-positive neurons were Pax6-positive, $n = 683$, three animals), suggesting a tight correlation between Pax6 and dopaminergic periglomerular neurons. Most dopaminergic periglomerular neurons also contained GABA ($79 \pm 3\%$, $n = 293$ cells, two animals), and all of them also expressed



Pax6. In contrast, very few Pax6-positive neurons in the glomerular layer were colabeled with calretinin ($2 \pm 1\%$ of Pax6-positive cells; $n = 361$ cells, one animal) or with calbindin ($10 \pm 1\%$ of Pax6-positive cells; $n = 437$ cells, two animals). Taken together, these data suggest that Pax6 is regulated dynamically within the SEZ-RMS pathway: first, Pax6 is upregulated in most neuroblasts along the RMS but later is downregulated during neuronal differentiation in most neurons, except in the dopaminergic neurons of the glomerular layer.

The expression of the transcription factor Olig2 did not overlap with Pax6 ($n = 221$, two animals; see also ref. 19) and showed the opposite rostrocaudal gradient: $18 \pm 4\%$ of DAPI-positive cells were Olig2-immunopositive in the SEZ ($n = 341$, two animals), whereas only $2 \pm 1\%$ ($n = 412$, two animals) of the DAPI-positive cells in the center of the RMS were Olig2-positive (**Fig. 1k,l**). In contrast to Pax6, the number of Olig2-positive cells did not increase again, and we did not detect any Olig2-immunopositive neurons within the olfactory bulb ($n = 255$, two animals). Olig2 hardly ever co-localized with PSANCAM or DCX (SEZ: $< 1\%$, $n = 181$; RMS, $n = 123$; two animals each) or with GFAP ($< 1\%$ in SEZ, $n = 120$; RMS, $n = 88$; two animals each). Thus, Olig2 is expressed exclusively in type C transit-amplifying precursors in the SEZ, consistent with our previous data¹⁹.

The role of Pax6 and Olig2 in adult neural precursors

Next, we examined the cell-autonomous function of Pax6 and Olig2 by the use of replication-incompetent retroviral vectors that allow the manipulation of gene expression in few progenitor cells and in all of their respective progeny within a normal environment. Given the pronounced gradient of Pax6 and Olig2 in the SEZ-RMS system, we decided to compare the manipulation of these transcription factors at both positions. When injections of viral vectors containing GFP (green fluorescent protein)¹⁹ (see Methods) were stereotactically targeted to the SEZ^{7,20,21}, $95 \pm 2\%$ of all GFP-positive cells were still located close to the SEZ 3 d after injection, and only $5 \pm 2\%$ were detected at some distance, within the RMS ($n = 45$, one animal; **Fig. 2a,b**; for 7 d after injection, see **Fig. 2e,f**). When the injection coordinates were modified

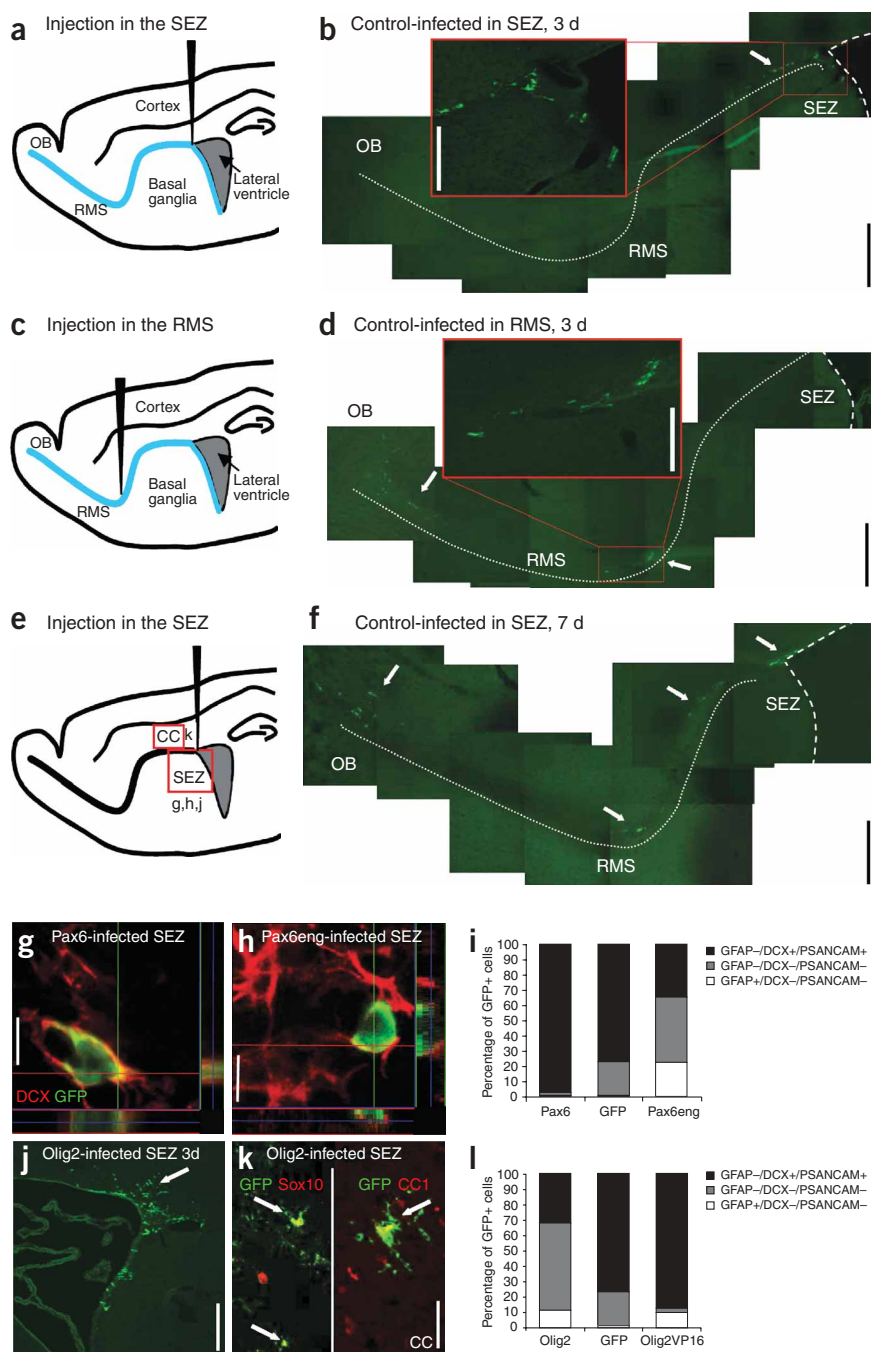


Figure 2 Functional analysis of the transcription factors Pax6 and Olig2 in adult neurogenesis. (**a,c,e**) Schematic drawings illustrating the injection sites (RMS, SEZ) of the viral vectors. Red boxes in **e** indicate the localization of the micrographs in **g,h,j,k**. (**b,d,f**) Micrographs depicting the localization of GFP-positive cells at different times after injection into the SEZ (**b,f,j**) or RMS (**d**). Insets (red) in **b** and **d** show GFP-positive cells in higher magnification. Arrows in **b,d,f,j** indicate GFP-positive cells. (**g,h,j,k**) Micrographs of double immunostaining in sagittal sections of the adult mouse SEZ (**g,h,j**) and corpus callosum (**j,k**) 7 d after vector injection (arrows indicate double-positive cells). Panel **h**: GFAP immunostaining, red; GFP, green. Pax6eng: Pax6engrainedIRESGFP virus. Micrographs below and to the right of **g,h** show z-stacks of the confocal pictures along the y-axis (right) and the x-axis (left). (**i,l**) Histograms summarizing quantification of GFP-positive SEZ cells 7 d after injection of the viral vectors indicated on the x-axis. Note that Pax6 plays a role in neurogenesis, whereas Olig2 promotes the generation of marker-negative cells. Scale bars: **b,d,f**, 500 μ m (insets: 200 μ m); **g,h**, 8 μ m; **j**, 180 μ m; **k**, 40 μ m.

of *Olig2* was removed (see Methods) or replaced with the transactivator domain VP16 (*Pax6*IRESGFP or *Olig2*IRESGFP; ref. 23). Previous *in vivo* and *in vitro* studies have shown that these constructs produce the opposite effect from the wild-type transcription factor, suggesting that they indeed antagonize the function of Pax6 and Olig2, respectively^{19,22–24}. We performed further control experiments that compared the dominant-negative constructs with loss-of-function conditions (**Supplementary Fig. 1**). These experiments showed that dominant-negative constructs are specific and exert no effects in cells that do not endogenously express the respective transcription factor.

When virus with wild-type Pax6 (ref. 19) was injected into the adult SEZ (**Fig. 2g,i**), a larger number of Pax6-transduced precursors progressed to the neuronal lineage (DCX-immunopositive; $n = 281$, three hemispheres, three animals) than in those infected with the control virus ($n = 183$, four hemispheres, three animals; $P < 0.001$) 1 week after injection

to target the central RMS, we reliably observed the vast majority of GFP-positive cells 3 d after injection migrating forward in the RMS ($72 \pm 1\%$ in the RMS outside the olfactory bulb, $21 \pm 5\%$ in the RMS inside the olfactory bulb) with only $6 \pm 1\%$ of cells apparently migrating backwards to the SEZ ($n = 66$, one animal; **Fig. 2c,d**). Thus, the targeted injection of viral vectors allows manipulation of gene expression locally at two distinct places of the SEZ-RMS system.

To manipulate the expression patterns of Pax6 and Olig2 in the SEZ and the RMS, we used vectors containing the wild-type forms of Pax6 or Olig2 and GFP mediated by the IRES sequence (*Olig2*IRESGFP)¹⁹. As dominant-negative constructs, we used *Pax6engrained*²², which contains the engrailed repressor domain instead of the normal transactivating domain of *Pax6*; for *Olig2*, the repressor domain

(**Fig. 2g,i**). Likewise, we observed a prominent reduction in the proportion of neuroblasts (to 42% of the control, $n = 100$, two hemispheres, two animals; $P < 0.001$) and a respective increase in other precursors in the SEZ 1 week after transduction with *Pax6engrained*IRESGFP vectors (**Fig. 2h,i**). We observed a comparable reduction of infected precursors assuming a neuronal precursor fate (DCX-positive, to $39 \pm 11\%$, $n = 83$, three hemispheres, two animals; **Supplementary Fig. 1**) compared with the control virus injections (control: $n = 70$, two hemispheres, two animals; $P < 0.05$) when we deleted Pax6 using Cre virus injection into mice in which the N-terminal part including the paired domain of the Pax6 gene was flanked by *loxP* sites²⁵. Analyses of TUNEL staining performed 3 or 7 d after viral injection showed no differences in death of infected cells,

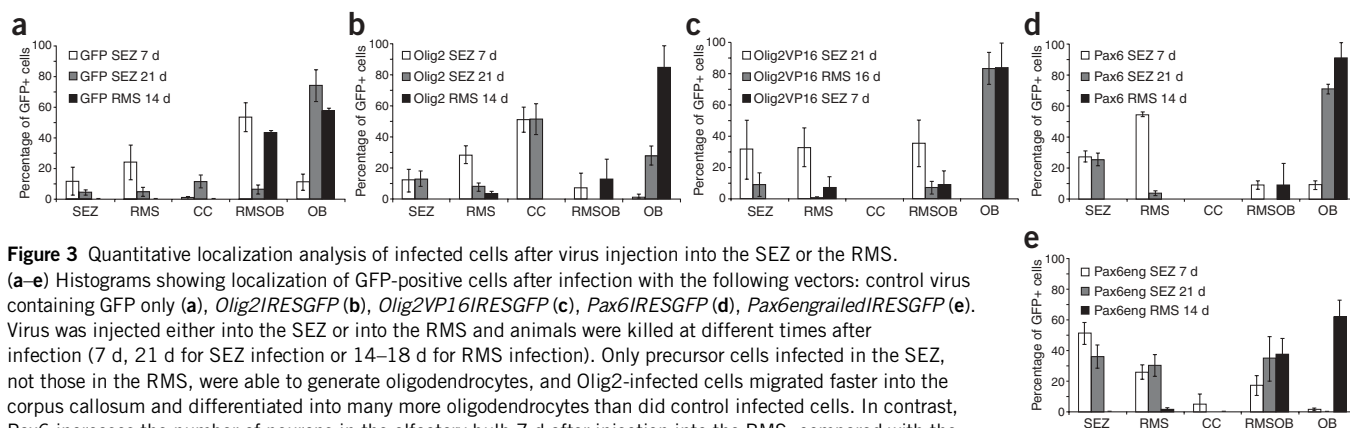


Figure 3 Quantitative localization analysis of infected cells after virus injection into the SEZ or the RMS. (a–e) Histograms showing localization of GFP-positive cells after infection with the following vectors: control virus containing GFP only (a), *Olig2*IRESGFP (b), *Olig2VP16*IRESGFP (c), *Pax6*IRESGFP (d), *Pax6engrailed*IRESGFP (e). Virus was injected either into the SEZ or into the RMS and animals were killed at different times after infection (7 d, 21 d for SEZ infection or 14–18 d for RMS infection). Only precursor cells infected in the SEZ, not those in the RMS, were able to generate oligodendrocytes, and *Olig2*-infected cells migrated faster into the corpus callosum and differentiated into many more oligodendrocytes than did control infected cells. In contrast, *Pax6* increases the number of neurons in the olfactory bulb 7 d after injection into the RMS, compared with the control virus injection (compare a and d, black bars), whereas *Pax6engrailed* virus reduces the proportion of neurons in the olfactory bulb upon injection into the SEZ (white and gray bars in e). Cells infected with the *Pax6engrailed* virus in the SEZ remained in the SEZ to a larger extent, and virtually no cells reach the layers of the olfactory bulb. Thus, endogenous *Pax6* function seems to be required for neuroblast specification and migration.

suggesting that selective cell death of precursor subtypes does not play a major role in the observed changes. These results implicate *Pax6* in the regulation of adult neurogenesis, supposedly by means of its coordinated effects on cell proliferation and cell fate as observed in cerebral cortex development^{26,27}.

Olig2 exerted effects opposite to *Pax6* on precursor cells in the adult SEZ. *Olig2* overexpression resulted in a decrease in neuronal precursors immunoreactive for DCX (Fig. 2i; to $35 \pm 3\%$ of control; $n = 181$, three hemispheres, three animals, $P < 0.001$) to levels comparable to those achieved with *Pax6engrailed* expression (compare Fig. 2i and Fig. 2l). However, the decrease in neuronal precursors resulted mostly from an increase in precursors negative for both GFAP and DCX: supposedly the transit-amplifying type C cells. Indeed, consistent with the expression of endogenous *Olig2* exclusively in this precursor type, expression of its dominant-negative form, *Olig2VP16*, virtually abolished this precursor cell type (Fig. 2l). Similar effects were obtained with a loss-of-function construct containing only the *Olig2bHLH* domain but no repressor domain (Supplementary Fig. 1). Thus, *Olig2* is necessary and sufficient to specify transit-amplifying precursors in the SEZ. Taken together, these data support functional roles as deduced from protein localization: *Olig2* is crucial for the specification of transit-amplifying fate, whereas *Pax6* is important for neuronal fate.

Olig2 promotes adult oligodendroglialogenesis

When overexpressing *Olig2*, we also noted a prominent emigration from the SEZ-RMS system 3 d after viral injection (Fig. 2j), whereas no cells infected with the control virus were located outside the SEZ-RMS system at this stage ($<1\%$, $n = 45$, one animal; see above). However, 7 d post-injection in control virus injections, some descendants of the infected cells had left the RMS and migrated to the corpus callosum (Fig. 3a, $1 \pm 1\%$, $n = 201$, four hemispheres, three animals); this reached $11 \pm 4\%$ ($n = 242$, four hemispheres, three animals) 21 d after injection. These cells were identified as oligodendrocytes or their precursors by CC1 or Sox10 immunoreactivity, respectively. One week after wild-type *Olig2* virus injection into the SEZ, $50 \pm 9\%$ of all infected cells ($n = 207$, three hemispheres, three animals, $P < 0.001$ compared to control) were detected within the corpus callosum (Fig. 3b) and had acquired oligodendrocyte identity (Fig. 2k). The increase in oligodendroglialogenesis was accompanied by a decrease in neuronal precursors as well as in the proportion of neurons reaching the olfactory bulb (Figs. 2l and 3b), suggesting that neurons and

oligodendrocytes originate from the same progenitors in the SEZ rather than from direct transduction of oligodendrocyte precursors in the corpus callosum. Indeed, the maintenance of *Olig2* expression interferes with neuronal differentiation, as previously shown^{28,29}. Consistent with a role for *Olig2* in the endogenous low degree of oligodendroglialogenesis, this was completely blocked after injection of *Olig2VP16* virus in the SEZ (Fig. 3c).

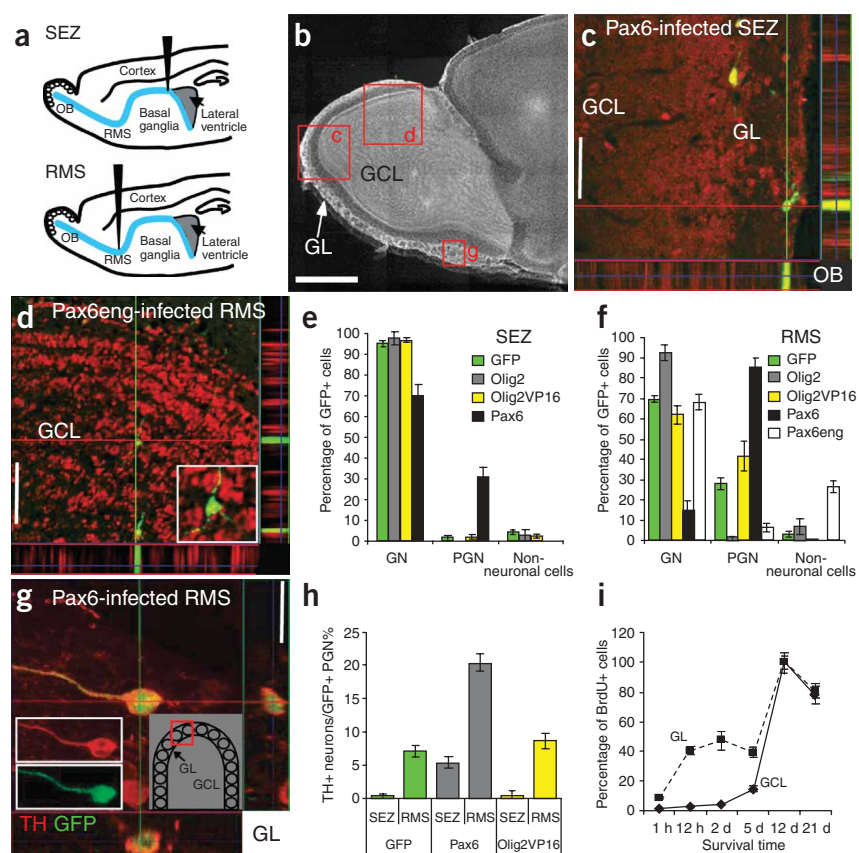
RMS precursors are restricted toward a neuronal fate

Given the gradient of these transcription factors along the RMS, we next performed the same functional analysis by injection into the RMS (Fig. 2c,d). These experiments showed differences in the cell-type specification at this position that intrigued us. When the *Pax6engrailed* virus was injected into the RMS, the effect on neurogenesis 7 d after injection was weaker than when the virus was injected into the SEZ (control: $94 \pm 1\%$ DCX-positive cells among GFP-positive cells, $n = 80$, two hemispheres, two animals; *Pax6engrailed*: $78 \pm 4\%$, $n = 80$, two hemispheres, two animals; Fig. 3e). Thus, precursors are further committed to the neuronal lineage within the RMS than in the SEZ, and this commitment is hardly reversible by *Pax6engrailed* transduction. Similarly, overexpression of *Olig2* in the RMS could not elicit oligodendrocyte generation ($n = 207$, five hemispheres, three animals Fig. 3b). Taken together, these data indicate that precursors in the RMS are further fate-restricted, and instead of promoting the generation of non-neuronal cells, both *Pax6engrailed* and *Olig2* transduction still resulted in a large number of cells progressing toward the neuronal lineage.

The role of *Pax6* in neuronal subtype specification

Next, we examined neuronal subtypes generated by precursors manipulated within the SEZ or the RMS 2–3 weeks after injection. First, we compared the neuronal subtypes generated by cells infected with the GFP control virus in the SEZ or the RMS. Consistent with previous data^{4,20,21}, most SEZ precursors gave rise to GFP-positive neurons in the GCL ($94 \pm 2\%$, $n = 316$, four hemispheres, three animals) and few neurons were detected in the glomerular layer ($2 \pm 1\%$, Fig. 4e). Notably, control virus injection into the RMS resulted in a significantly larger proportion of periglomerular neurons among all GFP-positive cells in the olfactory bulb ($30 \pm 3\%$, $n = 379$, three hemispheres, two animals; Fig. 4f; $P < 0.001$ compared with control). These results suggest a new concept: namely, that many periglomerular neurons originate at a rostral position of the SEZ-RMS system. However, the

Figure 4 Functional analysis of Pax6 and Olig2 in the specification of neuronal subtypes in adult neurogenesis. **(a)** Injection sites, as in **Figure 2**. **(b)** Micrograph of the olfactory bulb. Red boxes: position of the micrographs in **c,d,g**. **(c,d,g)** GFP-positive neurons in the olfactory bulb with micrographs of z-stacks of the confocal pictures along the y-axis (right) and the x-axis (left). Inset in **d**: higher magnification. **c** depicts a double-stained periglomerular neuron in the glomerular layer (NeuN, red; GFP, green). **d** shows double-stained neurons in the granule cell layer (GCL) (NeuN, red; GFP, green). **(e,f)** Percentage of GFP-positive cell types in the olfactory bulb 21 d after injection of viral vectors into the SEZ (**e**) or 14–16 d after injection into RMS (**f**). GN, granule neurons; PGN, periglomerular neurons. Note that Pax6 transduction increases the generation of periglomerular neurons located in the glomerular layer. **(g)** Micrograph of a GFP- and TH-double immunoreactive cell. **(h)** Percentage of TH-positive periglomerular neurons after viral vector injection into the SEZ (3 weeks survival) or RMS (2 weeks). Note that only RMS, but few SEZ precursors generate TH-positive periglomerular neurons (green) and that this fate is strongly promoted by Pax6 (gray), whereas blocking Olig2 function (Olig2VP16) has no effect (yellow). **(i)** Proportion of BrdU-labeled cells in glomerular layer (GL) and GCL of the olfactory bulb at different times after BrdU injection (y-axis). Scale bars: **b**, 100 μ m; **c**, 50 μ m; **e**, 150 μ m (inset, 30 μ m); **g**, 30 μ m.



majority of progenitor cells infected in the RMS ($70\% \pm 2$, $n = 379$, three hemispheres, two animals; **Fig. 4f**) were still granule neuron precursors. As most neuronal precursors in the RMS contain Pax6 ($64\% \pm 2$, $n = 235$, two animals), these data further support the idea that Pax6 is also contained in granule neuron precursors.

Given that Pax6 persisted in postmitotic periglomerular neurons, whereas it was downregulated in postmitotic granule neurons, we next examined whether the retrovirally mediated persistence of Pax6 protein in olfactory bulb neurons would be sufficient to instruct the differentiation towards the periglomerular neuron fate. Indeed, Pax6 overexpression in RMS precursors was sufficient to convert the fate of $70 \pm 2\%$ of granule neurons in the control injections to a periglomerular neuron fate, with almost all of the neurons overexpressing Pax6 located in the glomerular layer ($85 \pm 5\%$, $n = 90$, three hemispheres, three animals, $P < 0.001$ compared with control; **Fig. 4f**). These data implicate Pax6 as a key determinant for periglomerular neuron neuronal subtype specification. Indeed, injection of Pax6engrained-IRESGFP virus into the RMS significantly reduced the proportion of periglomerular neurons normally generated there to less than one-third of the value obtained in control virus injections ($6 \pm 2\%$, $n = 141$, four hemispheres, three animals, **Fig. 4d,f**, $P < 0.001$ compared to control), suggesting that the maintenance of endogenous Pax6 expression in RMS precursor cells is required to progress towards a periglomerular neuron subtype. Pax6 virus injection into the SEZ was also sufficient to instruct periglomerular neuron fate ($30 \pm 5\%$, $P < 0.001$, compared with control, $n = 80$, three hemispheres, three animals, **Fig. 4c,e**), albeit to significantly lower levels than in the RMS injections ($P < 0.001$ comparing Pax6 virus injection into SEZ and RMS). These data may be explained by SEZ precursors being biased,

either by intrinsic or extrinsic factors, toward a granule neuron fate, suggesting a new concept of early neuronal subtype specification during adult neurogenesis.

Given the close correlation of Pax6 and TH immunoreactivity, we next examined whether Pax6 overexpression was also sufficient to induce differentiation of periglomerular neurons toward a dopaminergic transmitter phenotype. Indeed, 2–3 weeks after viral injection, the number of TH-positive periglomerular neurons was significantly greater after Pax6 transduction than after control injections, in both SEZ and RMS (**Fig. 4h**). Since it is well established that the final acquisition of TH immunoreactivity for newborn neurons takes several weeks³⁰ and requires synaptic contacts³¹, we also examined TH immunoreactivity 3 months after viral injection. By then, $33 \pm 6\%$ of all GFP-positive periglomerular neurons resulting from control virus injections in the RMS had acquired TH immunoreactivity ($n = 123$, three hemispheres, two animals). Notably, about one-half of all GFP-positive periglomerular neurons had acquired TH immunoreactivity 2–3 months after injection of Pax6 virus into the RMS (**Fig. 4g**; $48 \pm 1\%$, $n = 116$ GFP-positive periglomerular neuron from four hemispheres, three animals; $P < 0.05$ as compared to control). Thus, Pax6 overexpression significantly promotes the acquisition of a dopaminergic transmitter phenotype in adult neurogenesis.

In the RMS injections, Olig2 was able to interfere with the differentiation of periglomerular neurons (**Fig. 4f**; $n = 373$, four hemispheres, two animals, $P < 0.001$ compared to control). In contrast, Olig2VP16 expression exerted no significant effects on neuronal subtype specification in the RMS (**Fig. 4e,f**), further supporting the idea that it does not exert non-specific effects on precursors devoid of endogenous Olig2, as precursors in the RMS are (see above). As Olig2 is

not expressed in RMS precursors, we wondered whether the ectopic expression by Olig2 virus might exert its effects by downregulation of Pax6. Indeed, few Olig2-infected precursor cells in the RMS expressed Pax6 7 d after infection (Olig2IRESGFP: $19 \pm 1\%$, $n = 99$, one hemisphere, one animal), compared with a majority of Pax6-positive cells ($80 \pm 3\%$, $n = 163$, one hemisphere, one animal) after control virus injection.

Injections of Olig2- or Olig2VP16-containing viruses into the SEZ did not elicit any change in neuronal subtype specification (Fig. 4e; Olig2: $P > 0.05$ compared with control, $n = 176$, three hemispheres, three animals; Olig2VP16: $P > 0.05$ compared with control, $n = 406$, four hemispheres, three animals). Taken together, these data suggest that Olig2 does not exert a direct effect on neuronal subtypes, and that endogenous Olig2 expression in the immature type C precursors is not required for granule cell specification. These data, taken together with the results for Pax6, would imply that neuronal subtypes are specified at later stages in the lineage progression.

Distinct precursor niches in the SEZ and RMS

While the above data imply that Pax6 is a potent intrinsic fate determinant for the specification of periglomerular neuron versus granule neuron fate, our results also point to an important role of the local environment of the adult neural progenitor cells, as vector injections into the RMS resulted in a larger number of periglomerular neurons than injections into the SEZ. To test this idea further, we combined birthdating analysis by injection of the DNA synthesis marker BrdU with an analysis of the time needed for migration towards the olfactory bulb. If neurons were born close to the olfactory bulb, they should reach the olfactory bulb shortly after their birth, while those coming from more remote positions would need a longer time. Adult mice were injected once with BrdU and allowed to survive for increasing periods of time. In agreement with our viral vector injection data, most BrdU-positive cells in the olfactory bulb, 21 d after injection of BrdU, were localized in the GCL ($88.2 \pm 1.1\%$, $n = 5$ animals). In order to evaluate the dynamics of granule neuron and periglomerular neuron arrival to the olfactory bulb, we expressed their number after each survival period as a percentage of the final maximal density observed in the GCL and glomerular layer, respectively. Notably, 2 d after BrdU injection, the density of BrdU-positive cells markedly increased and reached its half-maximal value in the glomerular layer, but not in the GCL (Fig. 4i). Twelve days after BrdU injection, labeled cells reached their maximal density in both the glomerular layer and GCL (Fig. 4i), consistent with the time needed for migration from the SEZ^{7,21,30}. These experiments, together with the results obtained by viral vector injections, suggest that a considerable proportion of the newborn periglomerular neuron arise from the rostral part of the RMS close to the olfactory bulb.

DISCUSSION

Our results allow several crucial new insights into the mechanisms directing adult neural precursors toward specific lineages. First, we demonstrate a dual role of the transcription factor Pax6 in controlling both the degree of adult neurogenesis and periglomerular neuron fate. Pax6 was found to be crucial for generation of neuronal progenitors as well as for direction of neurons towards the glomerular layer and acquisition of a dopaminergic phenotype. This dual role is reflected in two expression waves of Pax6: it is upregulated in neuronal precursors of both periglomerular neurons and granule neurons in the SEZ-RMS system, and although granule neurons then downregulate Pax6 during their postmitotic differentiation, many periglomerular neurons maintain Pax6 expression as postmitotic neurons.

Second, our results suggest a new concept of a spatial separation of granule neuron and periglomerular neuron specification. Targeting retroviral lineage labeling to the SEZ or the RMS demonstrates the distinct bias of these precursors toward different neuronal subtypes. In particular, retroviral lineage tracing showed that SEZ precursors generate very few periglomerular neurons, whereas precursors located in the RMS give rise to a significantly larger population of periglomerular neurons. These data are consistent with BrdU birthdating experiments demonstrating that many periglomerular neurons are generated close to the olfactory bulb, whereas most granule neurons are generated at a considerable distance. These data suggest that in adult neurogenesis, different neuronal subtypes are specified at different positions.

The role of Olig2 and Pax6 in lineage progression

Adult SEZ precursors proceed from a less-committed state (stem cell, transit-amplifying cell) to a more-committed neurogenic state (neuroblasts, Fig. 1c). Our results implicate Olig2 and Pax6 as key factors in regulating this progression. Whereas Olig2 promotes a transit-amplifying precursor state, Pax6 opposes this role and promotes progression toward the neuronal lineage consistent with their role in neurosphere cultures^{17,19,32}. Pax6 deletion by injection of virus containing Cre or dominant-negative constructs into the SEZ blocks further Pax6 function that is necessary for progression of the neuronal lineage. When Pax6 function is blocked in the SEZ, almost all infected precursors deviate from the neuronal lineage: only 30% of precursors are DCX-positive 1 week after Pax6engrailed virus infection, and they never reach the olfactory bulb and differentiate into proper neurons. As similar results were obtained by genetic deletion of Pax6 in the SEZ, we conclude that neuronal specification is still reversible in almost all transduced SEZ precursors. This conclusion fits well with the idea that upregulation of Pax6 mediates an irreversible commitment to the neuronal lineage. Most neuronal precursors in the SEZ have very low levels of Pax6 not yet detectable by immunocytochemistry, but they soon become Pax6 immunoreactive within the RMS already adjacent to the SEZ. Most neuronal precursors migrating along the RMS express high levels of Pax6 and have obviously upregulated its crucial target genes for neurogenesis. At this stage, the fate of most neuronal precursors (70% of granule neuron precursors in the RMS) can no longer be reversed, with the exception of the periglomerular neuron precursors (30% of periglomerular neuron precursors in the RMS), which seem to be specified much closer to the olfactory bulb than the granule neuron precursors.

Consistent with this idea of progressive neuronal fate specification, high levels of Olig2 are able to convert neurogenesis to oligodendroglialogenesis only in the SEZ, and its expression is restricted to the transit-amplifying cells in the SEZ, not the RMS. Although cells with the antigenic characteristics of transit-amplifying precursors are detectable in the RMS, they are not Olig2-immunopositive, suggesting that this lineage differs intrinsically from the lineage in the SEZ. One interpretation is that these cells are also not bi-potent, as there is no oligodendroglialogenesis from RMS cells (Fig. 3), consistent with a role of Olig2 in bipotent cells during development^{19,29,32,33}. However, further analysis will have to clarify the extent to which the supposed type C cells in the RMS really have transit-amplifying identity^{16,17,34}. A small but significant lineage of oligodendrocytes was also apparent in control virus injections into the SEZ and was blocked by Pax6 overexpression, or loss of function or dominant-negative constructs of Olig2. Thus, our study demonstrates that adult SEZ cells commit to both neuronal and glial lineages. The difference between these two lineages seems to be determined by factors regulating Olig2. If Olig2 is downregulated, progression to the neuronal lineage can occur (see also

refs. 23,24,28,29,33), whereas its maintenance promotes an oligodendroglial fate (see Methods). Taken together, these results add two key molecular players to the regulation of adult neurogenesis and add an important set of descendants (namely, the oligodendrocytes) to the list of cell types generated by adult neural precursors.

Patterning of the SEZ-RMS system

From the results discussed above, two observations point to a regionalization of lineage and fate along the SEZ-RMS system. First, transit-amplifying precursors in the SEZ and RMS differ by their expression of *Olig2*, suggesting that these lineages diverge at an early stage of commitment. Second, many periglomerular neuron precursors become fate-restricted at a much more rostral position than granule neuron precursors. These data imply that at least a considerable proportion of granule neurons and periglomerular neurons, respectively, are specified at distinct locations along the SEZ-RMS system. Indeed, the spatially distinct specification and birth of some periglomerular neuron precursors was also apparent from two further independent sets of experiments. BrdU birthdating analysis shows that a significant proportion of periglomerular neurons arrives in the olfactory bulb only a few days after BrdU injection, whereas this takes about 2 weeks for granule neurons. These data may theoretically be explained by different speeds of cell migration, in which case the periglomerular neurons should migrate with 5–10× higher speed of migration (about 170–340 $\mu\text{m}/\text{hour}$)³⁵. However, retroviral lineage tracing of precursors in the SEZ shows very few periglomerular neurons (see also refs. 7, 20), arguing against the possibility that many periglomerular neurons are in the same lineage as granule neurons but become postmitotic at more rostral positions. In contrast, when control virus is injected into the central RMS, a significantly higher proportion of labeled newborn neurons became periglomerular neurons. These results indicate that there are laminar differences between the fate of cells originating in the central RMS and those originating in the SEZ. However, some periglomerular neurons also originate in the SEZ³⁶, and it will be important to identify their specific phenotype.

Neural subtype specification by Pax6

During development, the local environment specifies fate by regulating intrinsic determinants. Our results implicate Pax6 in such a role, as granule neurons downregulate Pax6 during neuronal differentiation within the olfactory bulb, whereas Pax6 is maintained in the TH- and calbindin-positive subset of periglomerular neurons. We have confirmed the importance of the late expression of Pax6 in a specific neuronal sublineage at the functional level, as retroviral transduction of Pax6 allows maintenance of Pax6 expression, and this results in the almost complete conversion of all precursors in the RMS towards a periglomerular neuron fate. Thus, although granule neuron precursors in the RMS are firmly restricted to the neuronal lineage and can no longer be converted to a glial lineage, at least by the cues assessed here, their neuronal subtype is not yet fixed, and maintenance of Pax6 is sufficient to direct them to a periglomerular neuron fate. These data show that Pax6 is sufficient to instruct a periglomerular neuron fate in adult neurogenesis, even though SEZ precursors seem to be less amenable to this fate conversion.

Our results also suggest that endogenous Pax6 levels are important for periglomerular neuron specification. While Pax6engrailed transduction was not conclusive in this regard because neurogenesis of periglomerular neuron precursors was abolished altogether, *Olig2* virus injected into the RMS still allowed neuronal differentiation of most infected precursors (90%), although none acquired a periglomerular

neuron identity. These data suggest that the delayed downregulation of Pax6 in *Olig2*-infected precursors still allows neuronal differentiation but no longer allows the acquisition of a periglomerular neuron fate, for which a late phase of Pax6 expression seems to be crucial. These data are particularly exciting, as Pax6 imposes not only a laminar bias in the differentiation of olfactory bulb neurons, but also promotes the acquisition of a dopaminergic transmitter phenotype. The discovery of fate determination of dopaminergic neurons in the adult mammalian forebrain may be relevant for human patients, where some new neurons were also detected in the olfactory bulb³⁷, even though RMS has not been observed in human brains³⁸. Furthermore, an upregulation of TH-positive periglomerular neurons has been reported in Parkinson's patients, reflecting the apparent attempt to increase this neuronal phenotype³⁹. Thus, new insights into key regulators of endogenous adult neural stem cells are the key to diverting these cells towards a desired type.

METHODS

Retroviral vectors. The Pax6engrailed plasmid described in ref. 22 and the *Olig2bHLH* construct containing the amino acids 1–165 of the *Olig2* protein were inserted in sense orientation into the *EcoRI* unique restriction site of the retroviral vector *pMXIG*^{19,23} between the upstream long terminal repeat and the IRES sequence. The control virus (*CMMP* plasmid containing only GFP), as well as the Pax6, *Olig2* and *Olig2VP16* constructs and the viral production by gpg helper-free packaging cells were previously described¹⁹. Viral titers typically were 10^6 – 10^7 . Consistent with previous analysis, reliable coexpression of GFP and *Olig2* or Pax6 was observed 3, 7 and 21 d after viral transduction, with exception of neurons in the olfactory bulb that had downregulated *Olig2* 14 d after transduction. The lentiviral vectors (*LV-GFP* and *LV-Cre*) used are based on a recently described vector system⁴⁰ and were produced as described⁴¹.

Animals and stereotaxic injections. Injections of retroviral particles were done stereotactically on 9- to 10-week-old male mice as described⁷. All mouse lines were maintained on a C57BL/6J background. The following coordinates were used for virus injections (relative to bregma): for SEZ, anteroposterior = 0.75; mediolateral = 1.2; dorsoventral = 1.7; for RMS, anteroposterior = 3.3; mediolateral = 0.82; dorsoventral = 2.9. All experimental procedures were done in accordance with Society for Neuroscience and European Union guidelines and were approved by our institutional animal care and utilization committees.

Immunocytochemistry and BrdU birthdating. Immunostaining was carried out on 20- μm cryosections as described¹⁹; the following primary antibodies were used: anti-GFAP (Sigma, mouse IgG1), 1:200; anti-GFP (Clontech, rabbit), 1:1,000; anti-Sox10 (kindly provided by M. Wegner, Institute for Biochemistry, University Erlangen-Nurnberg; guinea pig), 1:1,000; anti-Pax6 (BABCO, rabbit), 1:500; anti-PSANCAM (kindly provided by P. Durbec, Institut de Biologie du Développement de Marseille; IgM), 1:500; anti-CC1 (Oncogene, IgG2B), 1:200; anti-DCX (Chemicon, guinea pig), 1:2,000; anti-NeuN (Chemicon, IgG1), 1:50; anti-TH (Pel-Freez, rabbit), 1:500; anti-Cre (Covance Research Product, rabbit), 1:5,000. Primary antibodies were detected by subclass-specific secondary antibodies labeled with FITC or TRITC or enhanced with the tyramide amplification kit (PerkinElmer). TUNEL staining was carried out using the cell death kit (Roche). Two- to three-month-old C57BL/6J mice were injected intraperitoneally with a DNA synthesis marker, 5-bromo-2'-deoxyuridine (BrdU; 50 mg/kg body weight, dissolved in 0.9% NaCl with 0.4 N NaOH). After different survival times following a single BrdU pulse, coronal sections of olfactory bulb were cut serially using a vibrating microtome (VT1000S, Leica) and detection and quantification of BrdU profiles were performed as previously described⁷. Stainings were analyzed with confocal microscopes (Leica, Zeiss).

Statistical analysis was done with the unpaired Student's *t*-test; *n* corresponds to the number of all cells analyzed. For the injections, the s.e.m. represents the variance between different injections into different animals;

that is, a single data point represents all of the GFP-positive cells counted in one animal. Usually two injections per animal were performed in both hemispheres.

Note: Supplementary information is available on the Nature Neuroscience website.

ACKNOWLEDGMENTS

We are particularly grateful to M. Nakafuku for the *pMXIG Olig2* and *pMXIG Olig2 VP16* constructs; N. Osumi for the *pMESpax6engrailed* construct; M. Wegner for the antisera directed against Sox10 and P. Durbec for providing PSANCAM antibodies. We also thank A. Bust, M. Öcalan and S. Ankri for excellent technical help. This work was supported by the Deutsche Forschungsgemeinschaft (M.G.) and by the Pasteur Institute (P.M.L., GPH no. 7, 'Stem cells') and the Centre National de la Recherche Scientifique and A.S. was supported by a postdoctoral fellowship from the Pasteur Institute and the Association Française Contre les Myopathies. R.A.-P. is supported by the Israel Science Foundation (401/02) and the German-Israeli Foundation for Scientific Research and Development.

COMPETING INTERESTS STATEMENT

The authors declare that they have no competing financial interests.

Received 7 March; accepted 13 May 2005

Published online at <http://www.nature.com/natureneuroscience/>

- Arvidsson, A., Collin, T., Kirik, D., Kokaia, Z. & Lindvall, O. Neuronal replacement from endogenous precursors in the adult brain after stroke. *Nat. Med.* **8**, 963–970 (2002).
- Nakatomi, H. *et al.* Regeneration of hippocampal pyramidal neurons after ischemic brain injury by recruitment of endogenous neural progenitors. *Cell* **110**, 429–441 (2002).
- Altman, J. Autoradiographic and histological studies of postnatal neurogenesis. IV. Cell proliferation and migration in the anterior forebrain, with special reference to persisting neurogenesis in the olfactory bulb. *J. Comp. Neurol.* **137**, 433–457 (1969).
- Luskin, M.B. Restricted proliferation and migration of postnatally generated neurons derived from the forebrain subventricular zone. *Neuron* **11**, 173–189 (1993).
- Lois, C. & Alvarez-Buylla, A. Long-distance neuronal migration in the adult mammalian brain. *Science* **264**, 1145–1148 (1994).
- Kosaka, K. *et al.* Chemically defined neuron groups and their subpopulations in the glomerular layer of the rat main olfactory bulb. *Neurosci. Res.* **23**, 73–88 (1995).
- Saghatelyan, A., de Chevigny, A., Schachner, M. & Lledo, P.M. Tenascin-R mediates activity-dependent recruitment of neuroblasts in the adult mouse forebrain. *Nat. Neurosci.* **7**, 347–356 (2004).
- Kosaka, T., Hataguchi, Y., Hama, K., Nagatsu, I. & Wu, J.Y. Coexistence of immunoreactivities for glutamate decarboxylase and tyrosine hydroxylase in some neurons in the periglomerular region of the rat main olfactory bulb: possible coexistence of gamma-aminobutyric acid (GABA) and dopamine. *Brain Res.* **343**, 166–171 (1985).
- Kosaka, K., Toida, K., Aika, Y. & Kosaka, T. How simple is the organization of the olfactory glomerulus?: the heterogeneity of so-called periglomerular cells. *Neurosci. Res.* **30**, 101–110 (1998).
- Jessell, T.M. Neuronal specification in the spinal cord: inductive signals and transcriptional codes. *Nat. Rev. Genet.* **1**, 20–29 (2000).
- Bertrand, N., Castro, D.S. & Guillemot, F. Proneural genes and the specification of neural cell types. *Nat. Rev. Neurosci.* **3**, 517–530 (2002).
- Marin, O. & Rubenstein, J.L. A long, remarkable journey: tangential migration in the telencephalon. *Nat. Rev. Neurosci.* **2**, 780–790 (2001).
- Rallu, M., Corbin, J.G. & Fishell, G. Parsing the prosencephalon. *Nat. Rev. Neurosci.* **3**, 943–951 (2002).
- Marshall, C.A., Suzuki, S.O. & Goldman, J.E. Gliogenic and neurogenic progenitors of the subventricular zone: who are they, where did they come from, and where are they going? *Glia* **43**, 52–61 (2003).
- Doetsch, F., Caille, I., Lim, D.A., Garcia-Verdugo, J.M. & Alvarez-Buylla, A. Subventricular zone astrocytes are neural stem cells in the adult mammalian brain. *Cell* **97**, 703–716 (1999).
- Garcia, A.D., Doan, N.B., Imura, T., Bush, T.G. & Sofroniew, M.V. GFAP-expressing progenitors are the principal source of constitutive neurogenesis in adult mouse forebrain. *Nat. Neurosci.* **7**, 1233–1241 (2004).
- Doetsch, F., Petreanu, L., Caille, I., Garcia-Verdugo, J.M. & Alvarez-Buylla, A. EGF converts transit-amplifying neurogenic precursors in the adult brain into multipotent stem cells. *Neuron* **36**, 1021–1034 (2002).
- Capela, A. & Temple, S. LeX/ssea-1 is expressed by adult mouse CNS stem cells, identifying them as nonependymal. *Neuron* **35**, 865–875 (2002).
- Hack, M.A., Sugimori, M., Lundberg, C., Nakafuku, M. & Götz, M. Regionalization and fate specification in neurospheres: the role of Olig2 and Pax6. *Mol. Cell. Neurosci.* **25**, 664–678 (2004).
- Belluzzi, O., Benedusi, M., Ackman, J. & LoTurco, J.J. Electrophysiological differentiation of new neurons in the olfactory bulb. *J. Neurosci.* **23**, 10411–10418 (2003).
- Petreanu, L. & Alvarez-Buylla, A. Maturation and death of adult-born olfactory bulb granule neurons: role of olfaction. *J. Neurosci.* **22**, 6106–6113 (2002).
- Yamasaki, T. *et al.* Pax6 regulates granule cell polarization during parallel fiber formation in the developing cerebellum. *Development* **128**, 3133–3144 (2001).
- Mizuguchi, R. *et al.* Combinatorial roles of olig2 and neurogenin2 in the coordinated induction of pan-neuronal and subtype-specific properties of motoneurons. *Neuron* **31**, 757–771 (2001).
- Novitsch, B.G., Chen, A.I. & Jessell, T.M. Coordinate regulation of motor neuron subtype identity and pan-neuronal properties by the bHLH repressor Olig2. *Neuron* **31**, 773–789 (2001).
- Ashery-Padan, R., Marquardt, T., Zhou, X. & Gruss, P. Pax6 activity in the lens primordium is required for lens formation and for correct placement of a single retina in the eye. *Genes Dev.* **14**, 2701–2711 (2000).
- Haubst, N. *et al.* Molecular dissection of Pax6 function: the specific roles of the paired domain and homeodomain in brain development. *Development* **131**, 6131–6140 (2004).
- Heins, N. *et al.* Glial cells generate neurons: the role of the transcription factor Pax6. *Nat. Neurosci.* **5**, 308–315 (2002).
- Lee, S.K., Lee, B., Ruiz, E.C. & Pfaff, S.L. Olig2 and Ngn2 function in opposition to modulate gene expression in motor neuron progenitor cells. *Genes Dev.* **19**, 282–294 (2005).
- Lu, Q.R. *et al.* Common developmental requirement for Olig function indicates a motor neuron/oligodendrocyte connection. *Cell* **109**, 75–86 (2002).
- Winner, B., Cooper-Kuhn, C.M., Aigner, R., Winkler, J. & Kuhn, H.G. Long-term survival and cell death of newly generated neurons in the adult rat olfactory bulb. *Eur. J. Neurosci.* **16**, 1681–1689 (2002).
- Brunjes, P.C. Unilateral naris closure and olfactory system development. *Brain Res. Brain Res. Rev.* **19**, 146–160 (1994).
- Gabay, L., Lowell, S., Rubin, L. & Anderson, D. Deregulation of dorsoventral patterning by FGF confers trilineage differentiation capacity on CNS stem cells *in vitro*. *Neuron* **40**, 485–499 (2003).
- Zhou, Q. & Anderson, D.J. The bHLH transcription factors OLIG2 and OLIG1 couple neuronal and glial subtype specification. *Cell* **109**, 61–73 (2002).
- Gritti, A. *et al.* Multipotent neural stem cells reside into the rostral extension and olfactory bulb of adult rodents. *J. Neurosci.* **22**, 437–445 (2002).
- Wichterle, H., Garcia-Verdugo, J.M. & Alvarez-Buylla, A. Direct evidence for homotypic, glia-independent neuronal migration. *Neuron* **18**, 779–791 (1997).
- Beech, R.D. *et al.* Nestin promoter/enhancer directs transgene expression to precursors of adult generated periglomerular neurons. *J. Comp. Neurol.* **475**, 128–141 (2004).
- Bedard, A. & Parent, A. Evidence of newly generated neurons in the human olfactory bulb. *Brain Res. Dev. Brain Res.* **151**, 159–168 (2004).
- Sanaï, N. *et al.* Unique astrocyte ribbon in adult human brain contains neural stem cells but lacks chain migration. *Nature* **427**, 740–744 (2004).
- Huisman, E., Uylings, H.B. & Hoogland, P.V. A 100% increase of dopaminergic cells in the olfactory bulb may explain hyposmia in Parkinson's disease. *Mov. Disord.* **19**, 687–692 (2004).
- Pfeifer, A., Brandon, E.P., Kootstra, N., Gage, F.H. & Verma, I.M. Delivery of the Cre recombinase by a self-deleting lentiviral vector: efficient gene targeting *in vivo*. *Proc. Natl. Acad. Sci. USA* **98**, 11450–11455 (2001).
- Pfeifer, A., Ikawa, M., Dayn, Y. & Verma, I.M. Transgenesis by lentiviral vectors: lack of gene silencing in mammalian embryonic stem cells and preimplantation embryos. *Proc. Natl. Acad. Sci. USA* **99**, 2140–2145 (2002).